Topological quantum matter with ultracold gases

Speaker: Sebastiano Peotta
Academy Research Fellow, Aalto University

Correlations in Topological Quantum matter, CTQM2022
Lammi, 7th September 2022

Outline

1) Quantum Hall effects and band structure invariants

2) The ultracold gas toolbox

3) Ultracold gas implementations of the integer quantum Hall effect

4) Towards the fractional quantum Hall effect with ultracold gases

1) Quantum Hall effects and band structure invariants

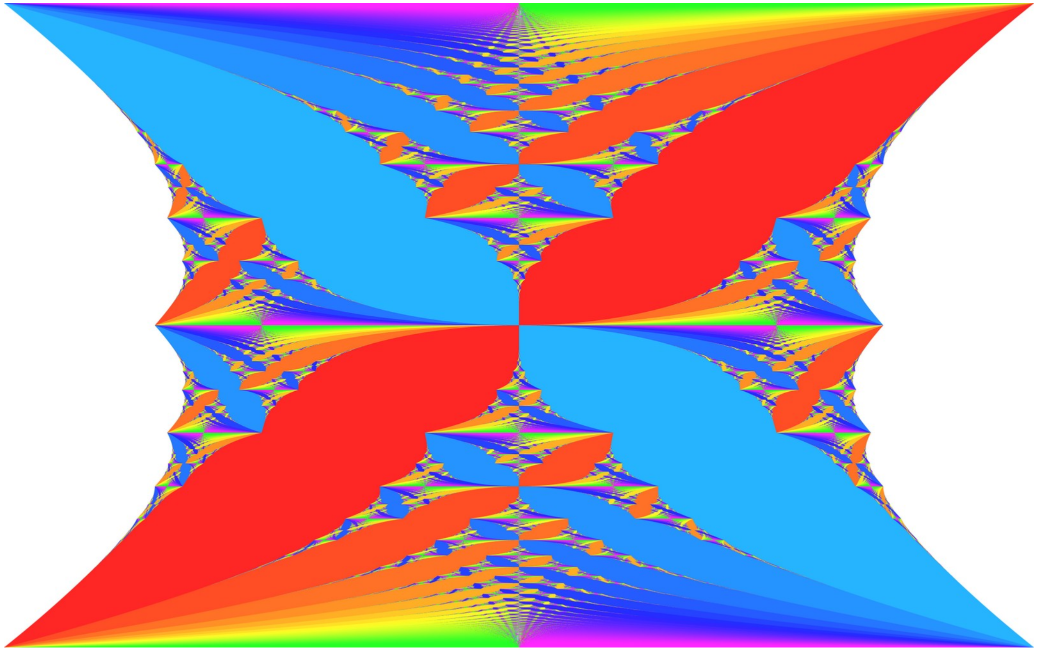

Quantum Hall effects

Integer and fractional quantum Hall effects (IQHE and FQHE) in ultrahigh-mobility GaAs/AlGaAs in two dimensional electrons gas

H. L. Stormer, Rev. Mod. Phys. **71**, 875 (1999)

- IQHE: topological band insulator
- FQHE: phase of matter with topological order

A. Bernevig and T. Neupert, arXiv:1506.05805

Topological order:
- Topological ground state degeneracy
- Fractionalized excitations
- Topological entanglement entropy

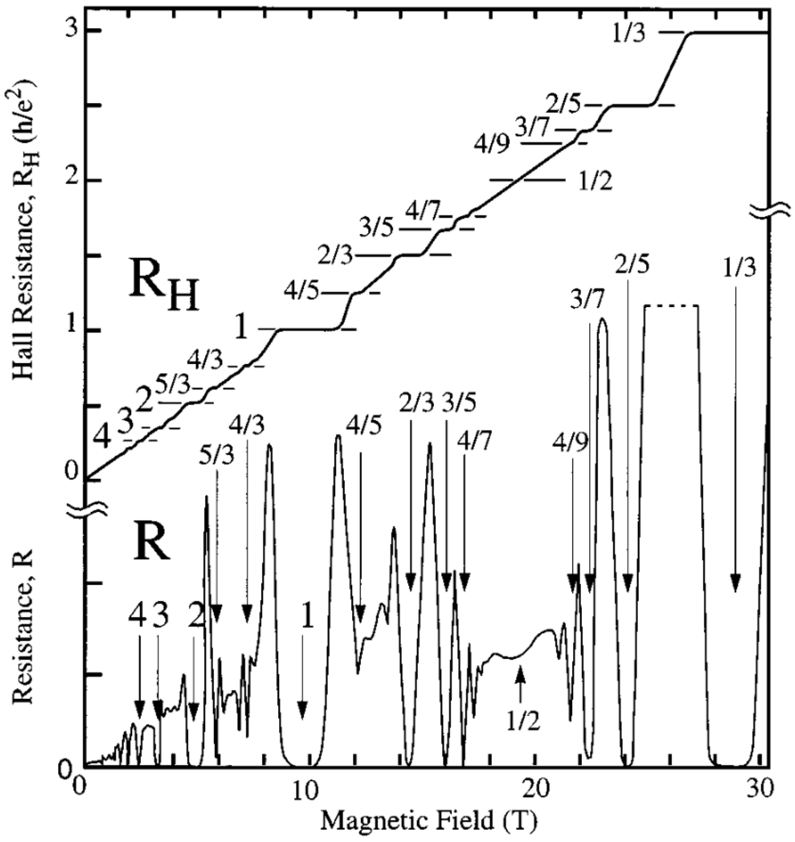

Band structure invariants

Topological band insulators are characterized by band structure invariants obtained from the wave functions of a noninteracting Hamiltonian

Discrete translational invariance → Bloch plane waves $\Psi_{n\mathbf{k}}(\mathbf{r}) = e^{i\mathbf{k}\cdot\mathbf{r}} g_{n\mathbf{k}}(\mathbf{r})$

Periodic Bloch functions $g_{n\mathbf{k}}(\mathbf{r}) = g_{n\mathbf{k}}(\mathbf{r} + \mathbf{a}_i)$ $\mathbf{a}_i$ lattice vectors

"Gauge" transformation $g_{n\mathbf{k}}(\mathbf{r}) \to e^{i\phi(\mathbf{k})} g_{n\mathbf{k}}(\mathbf{r})$

Band structure invariants = invariant under gauge transformations

Berry connection

$$\boxed{\mathbf{A}_n(\mathbf{k}) = i \langle g_{n\mathbf{k}} | \boldsymbol{\nabla}_{\mathbf{k}} g_{n\mathbf{k}} \rangle}$$

not an invariant $\mathbf{A}_n(\mathbf{k}) \to \mathbf{A}_n(\mathbf{k}) - \boldsymbol{\nabla}_{\mathbf{k}}\phi(\mathbf{k})$

transforms as the EM vector potential

Berry curvature and Chern number

Berry connection

Similar to a vector potential

$$\mathbf{A}_n(\mathbf{k}) = i\left\langle g_{n\mathbf{k}} \middle| \boldsymbol{\nabla}_{\mathbf{k}} g_{n\mathbf{k}} \right\rangle$$

not an invariant

Berry phase

Similar to a magnetic flux

$$\gamma_n(\mathcal{C}) = \oint_{\mathcal{C}} \mathrm{d}\mathbf{k} \cdot \mathbf{A}_n(\mathbf{k}) = \int_{\mathcal{S}} \mathrm{d}^2\mathbf{k}\, \Omega_n(\mathbf{k})\,, \quad \partial\mathcal{S} = \mathcal{C}$$

Berry curvature

Similar to a magnetic field along the z-axis (2D)

$$\Omega_n(\mathbf{k}) = \hat{z} \cdot \boldsymbol{\nabla}_{\mathbf{k}} \times \mathbf{A}_n(\mathbf{k})$$

Chern number

$$\boxed{C = \frac{1}{2\pi} \int_{\mathrm{B.Z.}} \mathrm{d}^2\mathbf{k}\, \Omega_n(\mathbf{k})}$$

The integral is over the Brillouin zone (B.Z.)

The Chern number C is always an integer!
Topological invariant proportional to the Hall conductance (IQHE)

Kubo-Chern formula $\quad \sigma_{\mathrm{H}} = \dfrac{e^2}{h} C$

D. Thouless, M. Kohmoto, M. Nightingale, and M. den Nijs, PRL **49** 405, (1982)

Quantum geometric tensor

A more comprehensive band structure invariant is the

Quantum Geometric Tensor

J. P. Provost and G. Vallee, Commun. Math. Phys. **76**, 289 (1980)

$$\begin{aligned}\mathcal{B}_{ij}(\mathbf{k}) &= 2\,\langle \partial_{k_i} g_{n\mathbf{k}}|\left(1-|g_{n\mathbf{k}}\rangle\langle g_{n\mathbf{k}}|\right)|\partial_{k_j} g_{n\mathbf{k}}\rangle \\ &= 2\,\mathrm{Tr}\left[P_n(\mathbf{k})\partial_{k_i}P_n(\mathbf{k})\partial_{k_j}P_n(\mathbf{k})\right] \quad \text{with} \quad P_n(\mathbf{k}) = |g_{n\mathbf{k}}\rangle\langle g_{n\mathbf{k}}|\end{aligned}$$

$$\mathrm{Re}\,\mathcal{B}_{ij}(\mathbf{k}) = \mathrm{Tr}\left[\partial_{k_i}P_n(\mathbf{k})\partial_{k_j}P_n(\mathbf{k})\right] = g_{ij}(\mathbf{k})$$ Quantum metric

$$\mathrm{Im}\,\mathcal{B}_{ij}(\mathbf{k}) = \epsilon_{ij}\Omega_n(\mathbf{k})$$ Berry curvature

Applications of the quantum metric

The quantum metric has found applications in many different contexts:

- Mobility gap in the integer quantum Hall effect (localization length): J. Bellissard, A. van Elst and H. Schulz- Baldes, J. Math. Phys. **35**, 5373 (1994), R. Resta, Eur. Phys. J. B **79**, 121 (2011)
- Localization functional for Wannier functions: N. Marzari et al., Rev. Mod. Phys. **84**, 1419 (2012); Marzari, N., and D. Vanderbilt, Phys. Rev. B **56**, 12847 (1997)
- Superfluidity in flat band systems: SP and P. Törmä, Nat. Comm. **6**, 8944 (2015); P. Törmä, SP and B. A. Bernevig, Nat. Rev. Phys. **4**, 528 (2022)
- Orbital magnetic susceptibility: Y. Gao et al., Phys. Rev. B **91**, 214405 (2015); F. Piéchon et al., Phys. Rev. B **94**, 134423 (2016)
- Current noise: T. Neupert, C. Chamon, and C. Mudry, Phys. Rev. B **87**, 245103 (2013)
- Fractional Chern insulators: R. Roy, Phys. Rev. B **90**, 165139 (2014); T. S. Jackson et al., Nat. Commun. **6**, 8629 (2015); Z. Liu and E. Bergholtz, arXiv:2208.08449
- …….

For an introduction see: Ran Cheng, arXiv:1012.1337

What about disorder?

Disorder is essential to explain the Hall conductance plateaus in the quantum Hall effects

The Kubo-Chern formula can be extended to the disordered case in the framework of noncommutative geometry J. Bellissard, A. van Elst and H. Schulz- Baldes, J. Math. Phys. **35**, 5373 (1994)

Fourier (Bloch-Floquet-Zak) transform

$$P_n(\mathbf{k}) = |g_{n\mathbf{k}}\rangle\langle g_{n\mathbf{k}}| \qquad \longleftrightarrow \qquad P = \theta(\mu - H)$$

$$\boldsymbol{\nabla}_{\mathbf{k}} A(\mathbf{k}) \qquad \longleftrightarrow \qquad -i[\mathbf{r}, A]$$

$$\int_{\mathrm{B.Z.}} \frac{\mathrm{d}^2\mathbf{k}}{(2\pi)^2} \mathrm{Tr}[A(\mathbf{k})] \qquad \longleftrightarrow \qquad \tau(A) = \lim_{\Lambda\to\infty} \frac{1}{|\Lambda|} \mathrm{Tr}_\Lambda[A_\Lambda]$$

$$C = \frac{1}{2\pi i} \int_{\mathrm{B.Z.}} \mathrm{d}^2\mathbf{k}\, \mathrm{Tr}\left[P_n(\mathbf{k})[\partial_{k_1} P_n(\mathbf{k}), \partial_{k_2} P_n(\mathbf{k})]\right] \qquad \longleftrightarrow \qquad C_{\mathrm{n.c.}} = 2\pi i \tau\big(P\big[[x, P], [y, P]\big]\big)$$

$$\sum_i \int_{\mathrm{B.Z.}} \frac{\mathrm{d}^2\mathbf{k}}{(2\pi)^2} g_{ii}(\mathbf{k}) = \int_{\mathrm{B.Z.}} \frac{\mathrm{d}^2\mathbf{k}}{(2\pi)^2} \mathrm{Tr}\left[|\boldsymbol{\nabla}_{\mathbf{k}} P_n(\mathbf{k})|^2\right] \qquad \longleftrightarrow \qquad \boxed{\tau\big(|[\mathbf{r}, P]|^2\big) = \lim_{\Lambda\to\infty} \frac{1}{|\Lambda|} \int_\Lambda \mathrm{d}^2\mathbf{r} \int \mathrm{d}^2\mathbf{r}'\, |\langle \mathbf{r}|P|\mathbf{r}'\rangle|^2 |\mathbf{r} - \mathbf{r}'|^2}$$

Localization length squared

The noncommutative Chern number $C_{\mathrm{n.c.}}$ is quantized if the localization length is finite (mobility gap)

Density of states and mobility gap

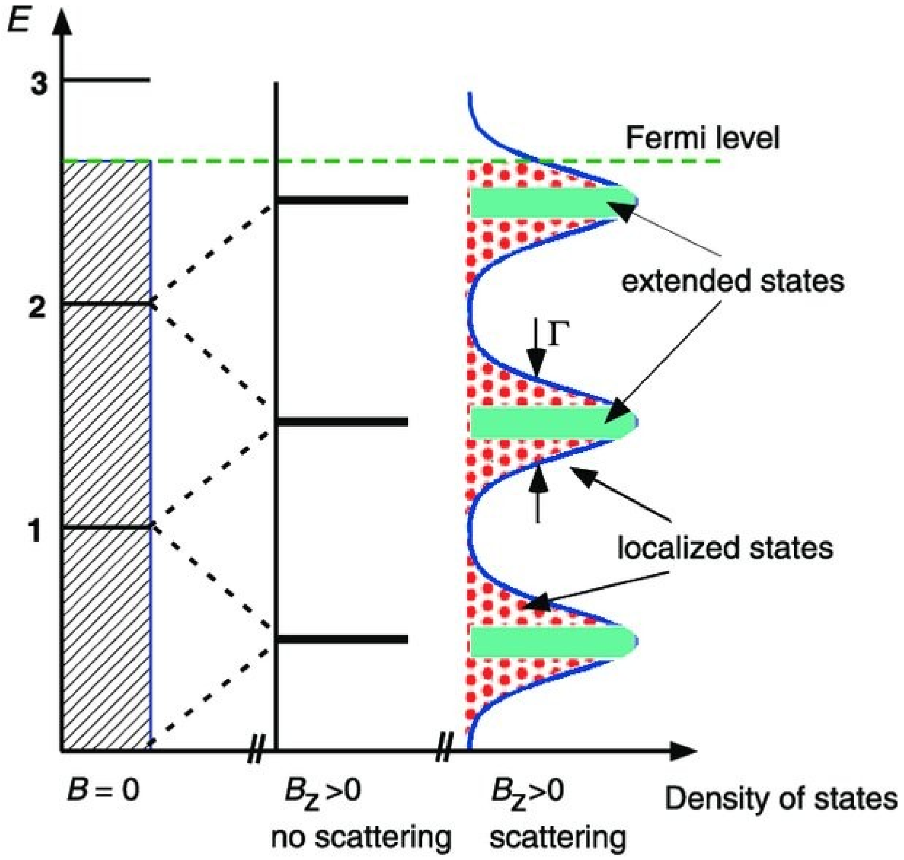

Extended states = diverging localization length

Localized states = finite localization length

Figure from B. Jeckelmann and B. Jeanneret, Rep. Prog. Phys. **64**, 1603 (2001)

New platforms

The quantum Hall effects are the blueprint for topological states of matter

Current challenges:

- FQHE at higher temperature and lower/zero magnetic field
- Novel topological phases (non-Abelian) → topological quantum computation
- Topological states of matter in systems other than quantum wells in semiconductors

Two promising candidate platforms
Z. Liu and E. Bergholtz, arXiv:2208.08449

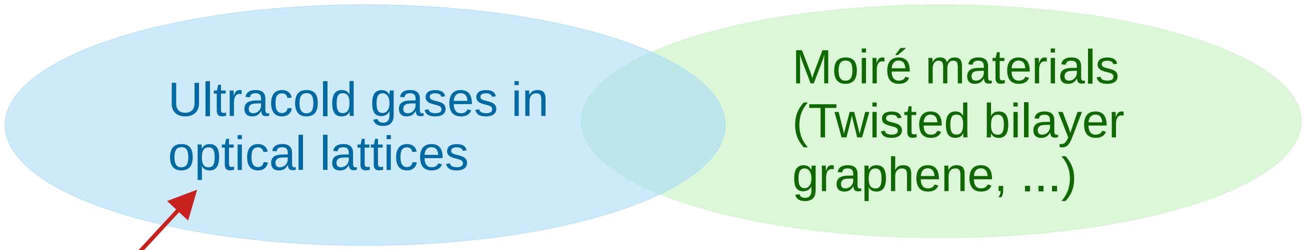

Focus of this talk

Ultracold gases can simulate moiré materials!

2) The ultracold gas toolbox

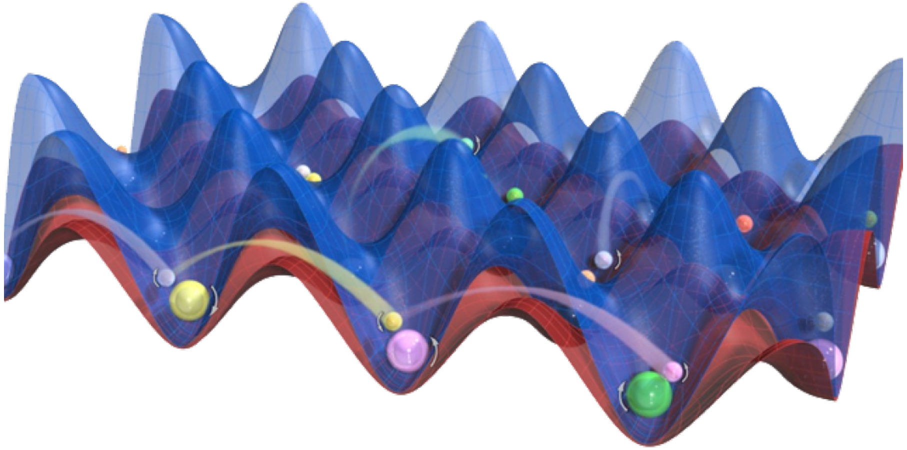

Ultracold gases: basics

Ultracold atoms: neutral atoms in vacuum trapped by laser light and magnetic fields

- Typical atoms: Rb, Cs, Na, K, Li, Yb, Sr, Er, Dy,…
- Density: from 10^{12} to 10^{15} cm^{-3}, interparticle spacing 0.1-1μm
- Temperature: down to fraction of nanoKelvin (nK)
- Entropy per particle: down to $S/N = 10^{-3}\,k_B$
- Atoms are in the ultracold regime when they reach degeneracy
- Bose-Einstein condensation (BEC) for bosonic atoms, degenerate Fermi gas for fermions

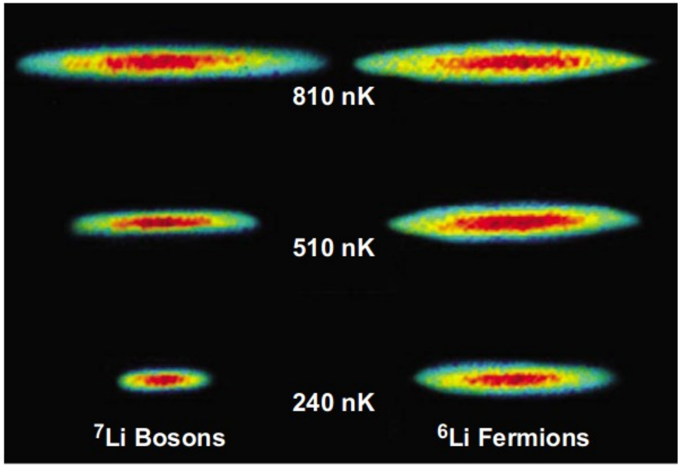

Ultracold gases in optical lattices have become a highly customizable platform for investigating quantum many-body physics Bloch, Dalibard, Zwerger, Rev. Mod. Phys. **80**, 885 (2009)

Optical lattices

Optical lattice = periodic potential for neutral atoms generated by laser standing waves

Single-particle Hamiltonian (continuum)

$$H_{\text{s.p.}} = -\frac{\hbar^2}{2m}\nabla^2_{\mathbf{r}} + V(\mathbf{r})$$

Periodic potential (cubic lattice)

$$V(\mathbf{r}) = V_x \sin^2(kx) + V_y \sin^2(ky) + V_z \sin^2(kz)$$

Low energy effective lattice Hamiltonian

$$\hat{\mathcal{H}} = -J \sum_{\langle \mathbf{i},\mathbf{j} \rangle} \hat{a}^\dagger_{\mathbf{i}} \hat{a}_{\mathbf{j}}$$

2D optical lattice

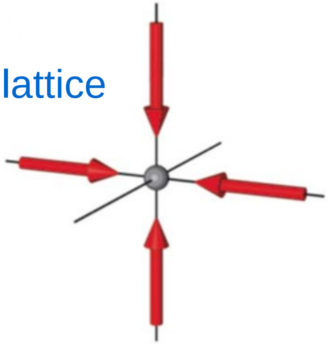

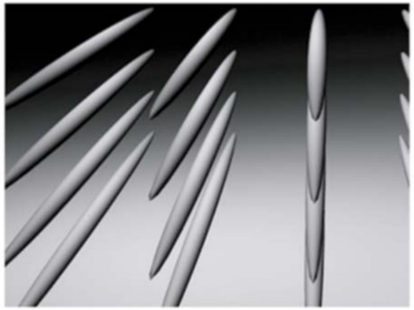

3D optical lattice

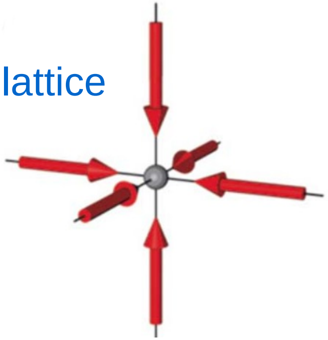

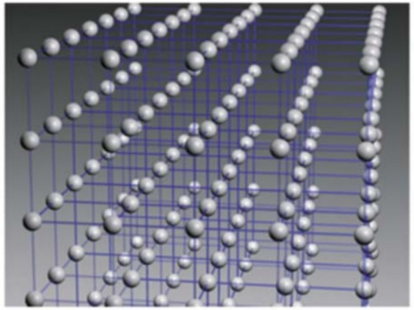

Superfluid-Mott insulator transition

Bose-Hubbard model with nearest-neighbour hopping

$$\hat{\mathcal{H}} = -J \sum_{\langle \mathbf{i},\mathbf{j} \rangle} a_{\mathbf{i}}^\dagger a_{\mathbf{j}} + \frac{U}{2} \sum_{\mathbf{i}} \hat{n}_{\mathbf{i}}(\hat{n}_{\mathbf{i}} - 1)$$

Condensate (BEC) wavefunction

$$|\Psi_N(U=0)\rangle = \frac{1}{\sqrt{N!}} \left(\frac{1}{N_c} \sum_{\mathbf{i}} \hat{a}_{\mathbf{i}}^\dagger \right)^N |\emptyset\rangle$$

Increasing U/J

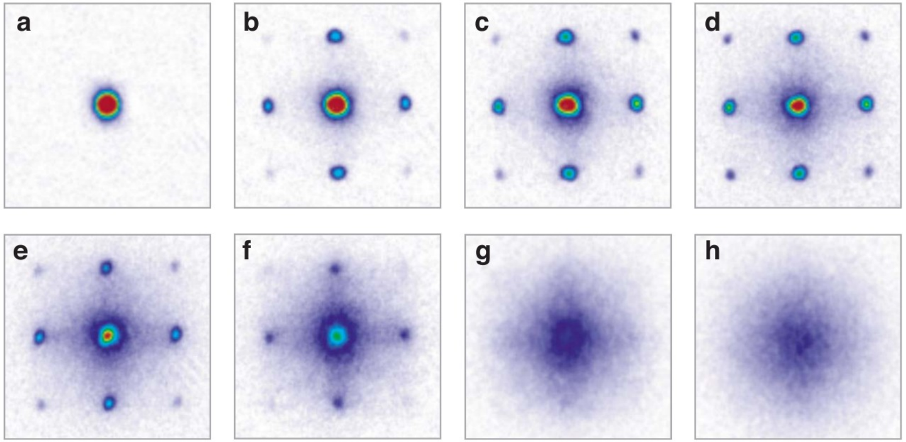

The effective mass is completely tunable in the range

$$m_{\mathrm{bare}} \leq m_{\mathrm{eff}} \propto J^{-1} \leq +\infty$$

M. Greiner, M. O. Mandel, T. Esslinger, T. Hänsch, and I.Bloch, Nature **415**, 39 (2002)

Increasing U/J

Mott insulator wavefunction

$$|\Psi_{N=N_c}(J=0)\rangle = \prod_{\mathbf{i}} \left(\hat{a}_{\mathbf{i}}^\dagger \right) |\emptyset\rangle$$

Engineering artificial gauge fields

Solid state systems: magnetic field and spin-orbit coupling → **gauge fields**

How to realize gauge fields for neutral atoms?

- Rotating traps
- Optical lattice shaking
- Laser-assisted tunneling
- Synthetic dimensions
- Optical flux lattices (theory)

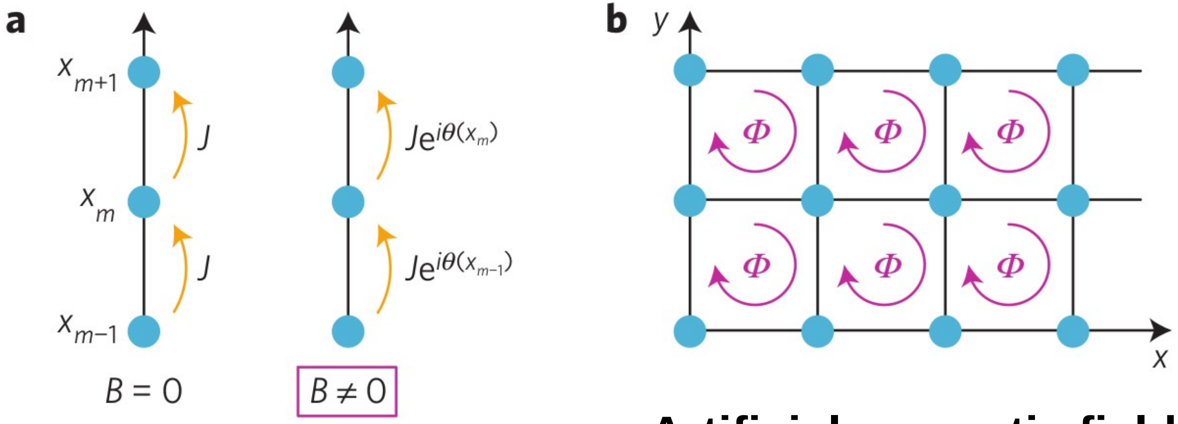

Peierls phase

Artificial magnetic field

Artificial gauge fields through lattice shaking

Original proposal: graphene irradiated by circularly polarized light, T. Oka and H. Aoki, PRB **79**, 169901 (2009)

Realized with ultracold atoms in a deformed hexagonal lattice, G. Jotzu, et al., Nature **515**, 237 (2014)

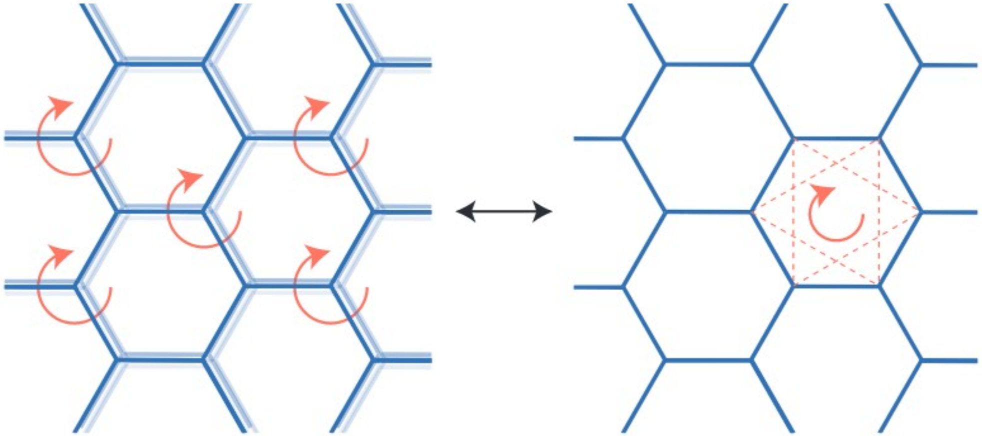

Circular shaking of an hexagonal lattice

Enhanced and complex next-nearest neighbor tunneling

Effective (Floquet) Hamiltonian from high-frequency expansion

$$\begin{aligned}\hat{H}_{\mathrm{F}} &\approx \hat{H}_{\mathrm{F}}^{(1)} + \hat{H}_{\mathrm{F}}^{(2)} \\ &= -J_{\mathrm{eff}}^{(1)} \sum_{\langle j,j' \rangle} \hat{a}_j^\dagger \hat{a}_{j'} \\ &\quad - J_{\mathrm{eff}}^{(2)} \sum_{\langle\langle j,j' \rangle\rangle} e^{-i\sigma_{j,j'}\theta} \hat{a}_j^\dagger \hat{a}_{j'}\end{aligned}$$

Haldane model
(to be introduced soon)

Laser-assisted tunneling in optical lattices

Laser-assisted tunneling has been used to realize the **Harper-Hofstadter model** (square lattice + uniform magnetic field)

[1] Aidelsburger et al., PRL **111**, 185301 (2013)
[2] Miyake et al., PRL **111**, 185302 (2013)
[3] Aidelsburger et al., Nat. Phys. **11**, 162 (2015)

Tunneling in the *x* direction is suppressed by the tilt Δ and restored by means of a two-phonon Raman process

Raman-assisted tunneling matrix elements are complex → **Peierls phase**

$$\hat{H} = -\sum_{m,n}\left(Ke^{-i\phi_{m,n}}\hat{a}^\dagger_{m+1,n}\hat{a}_{m,n} + J\hat{a}^\dagger_{m,n+1}\hat{a}_{m,n} + \mathrm{H.c.}\right)$$

$$\phi_{m,n} = \delta\mathbf{k}\cdot\mathbf{R}_{m,n} = (m\delta k_x + n\delta k_y)a$$

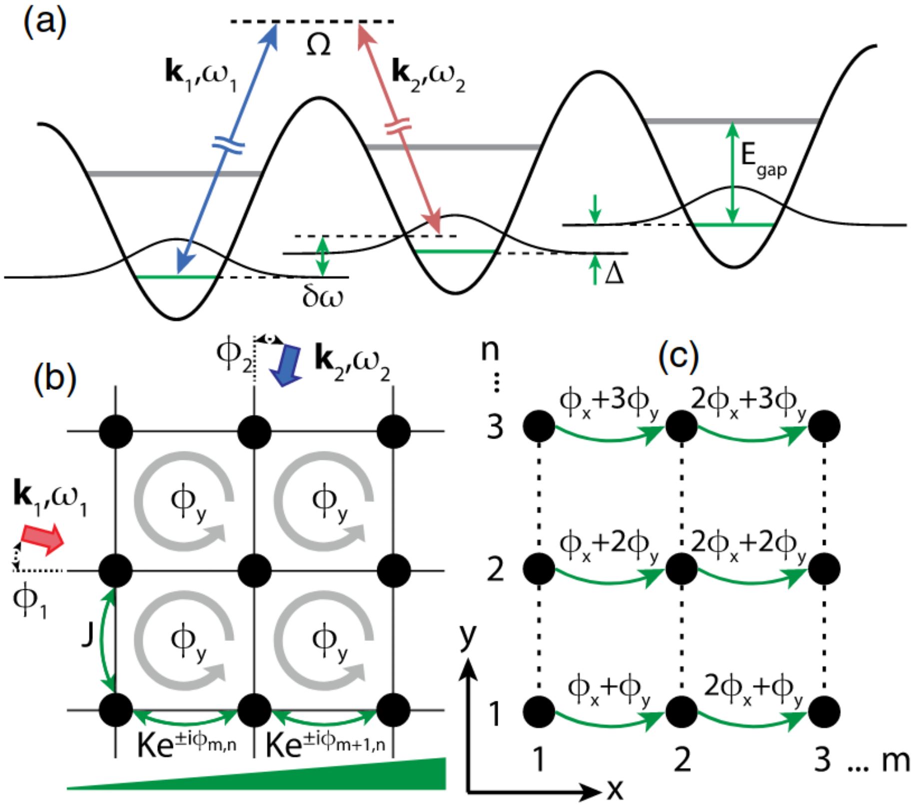

From Ref. [2]

Synthetic dimensions

Idea: the atom internal states (hyperfine states) become lattice sites aligned along a new fictitious spatial dimension A. Celi et al., PRL **112**, 043001 (2014)

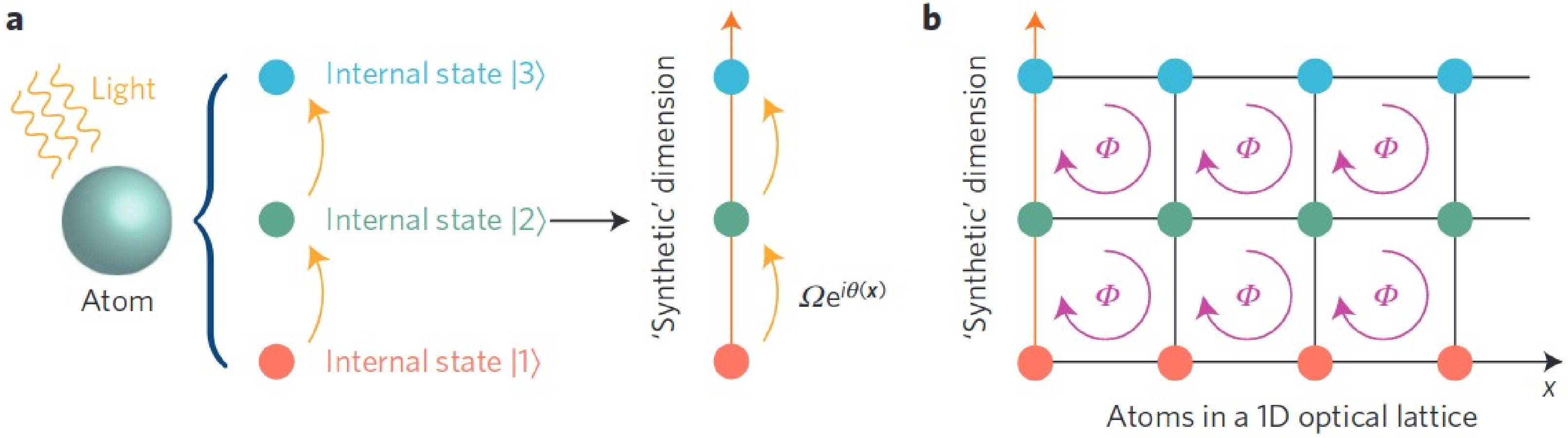

Hopping along the synthetic dimension is induced by resonant light or two-photon Raman transition

Advantages

- Single-site resolution along the synth. dim.
- Hard wall confinement along the synth. dim.
- Reduced heating, important for many-body effects

Simulating twisted bilayer graphene with ultracold atoms

Idea: use atom internal states to encode both layer and spin degrees of freedom (synthetic dimension)

Interlayer tunneling is introduced by a Raman transition

Raman detuning is modulated → modulated interlayer hopping

Periodicity of interlayer hopping is different from lattice periodicity → moiré pattern in interlayer hopping

Topological and quasiflat bands can be obtained, as in twisted bilayer graphene
T. Salamon et al., PRA **102**, 235126 (2020)

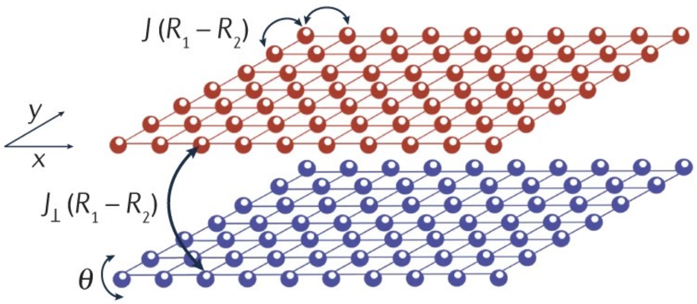

T. Salamon et al., PRL **125**, 030504 (2020)

P. Törmä, SP and B. A. Bernevig, Nat. Rev. Phys. **4**, 528 (2022)

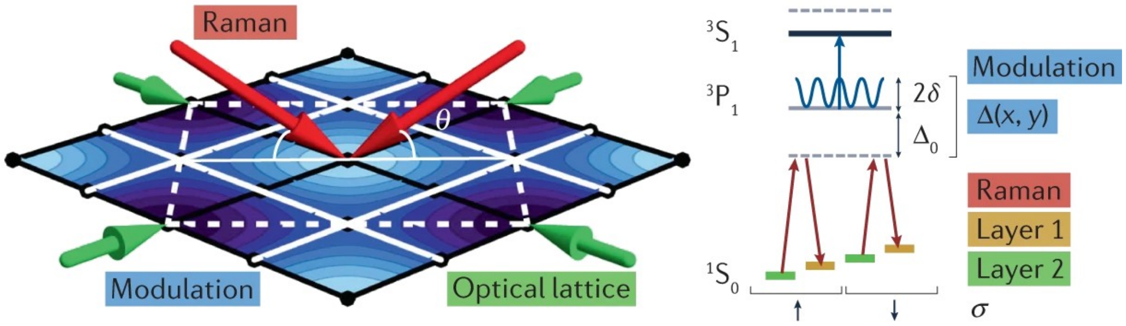

3) Ultracold atoms implementations of the integer quantum Hall effect

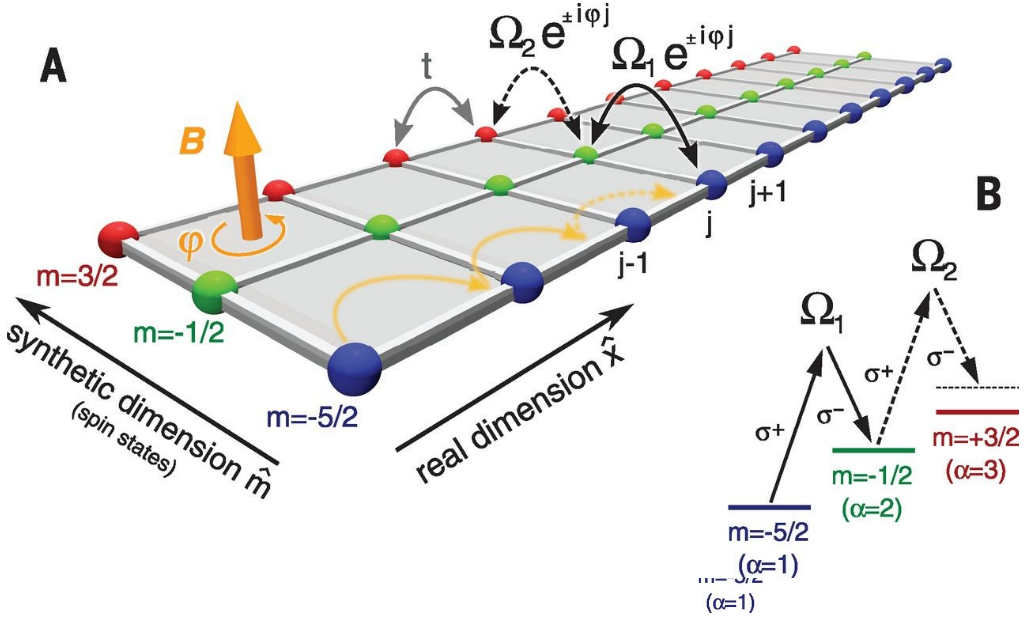

Haldane model: a prototype topological Hamiltonian

Simple two-orbital model with topologically nontrivial bands in the absence of a uniform magnetic field F. D. M. Haldane, PRL **61**, 2015 (1986)

$$\hat{\mathcal{H}} = -t_1 \sum_{\langle ik \rangle} (\hat{a}_i^\dagger \hat{b}_k + \text{H.c.}) - t_2 \left(\sum_{\langle\langle ij \rangle\rangle} e^{i\Phi_{ij}} \hat{a}_i^\dagger \hat{a}_j + \sum_{\langle\langle kl \rangle\rangle} e^{i\Phi_{kl}} \hat{b}_k^\dagger \hat{b}_l \right) + \Delta \sum_i \hat{a}_i^\dagger \hat{a}_i$$

nearest neighbor (NN) hopping

next NN hopping

sublattice energy difference

Breaks lattice inversion symmetry

$\Phi_{ij} = \Phi_{kl} = \Phi > 0$

for the next NN hoppings according to arrow directions

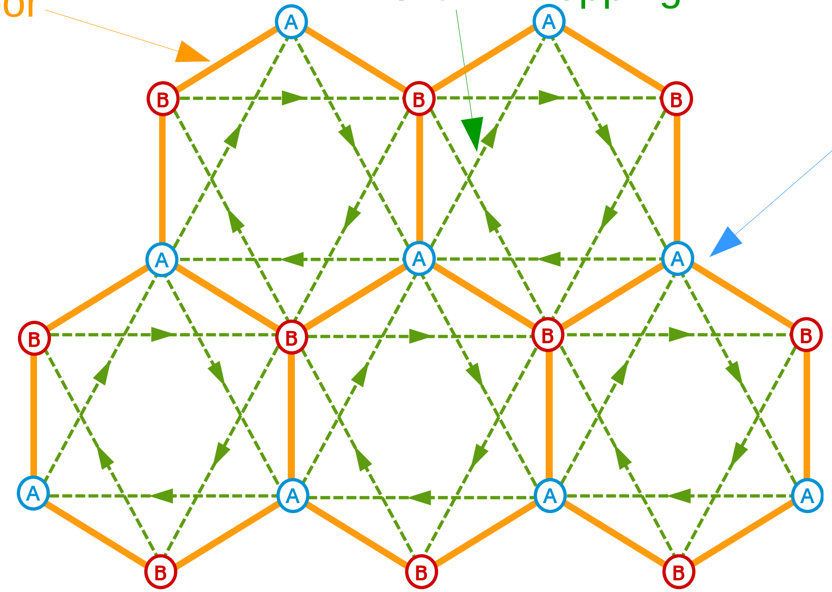

Breaks time-reversal symmetry, zero net magnetic flux

Example of anomalous Hall effect, Chern insulator

Phase diagram of the of the Haldane model

The Chern number changes when the band gap closes (Dirac point)

ν Chern number

sublattice energy difference

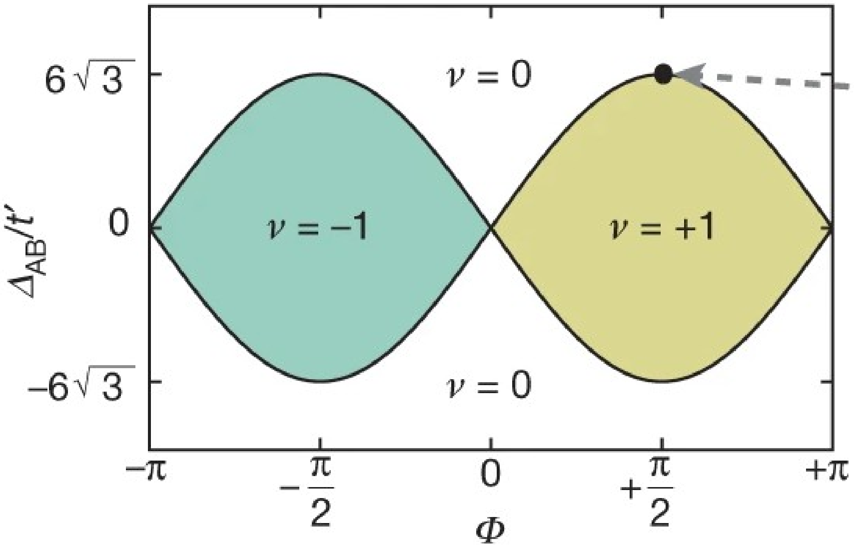

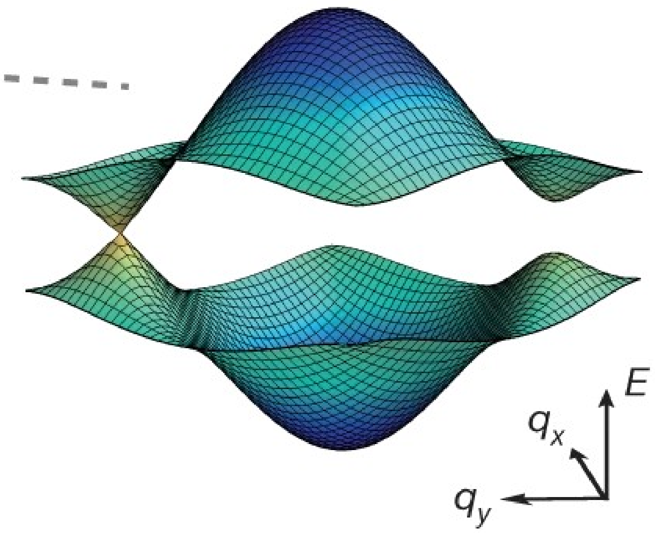

Peierls phase of next nearest neighbor hopping

Measuring the band topology: differential drift

Semiclassical equations of motion
for wavepacket center of mass

$$\dot{x} = \hbar^{-1}\partial_{k_x}\varepsilon(\mathbf{k}) - \dot{k}_y\Omega(\mathbf{k})$$
$$\dot{y} = \hbar^{-1}\partial_{k_y}\varepsilon(\mathbf{k}) + \dot{k}_x\Omega(\mathbf{k})$$
$$\hbar\dot{k}_x = -\partial_x V_{\text{trap}}(\mathbf{r})$$
$$\hbar\dot{k}_y = F_y - \partial_y V_{\text{trap}}(\mathbf{r})$$

$V_{\text{trap}}(\mathbf{r}) = \frac{1}{2}m(\omega_x x^2 + \omega_y y^2)$ trapping potential

$\Omega(\mathbf{k})$ Berry curvature

Berry curvature and trapping potential induce a drift orthogonal to the velocity in momentum space $\dot{\mathbf{k}} = \frac{\mathrm{d}\mathbf{k}}{\mathrm{d}t}$

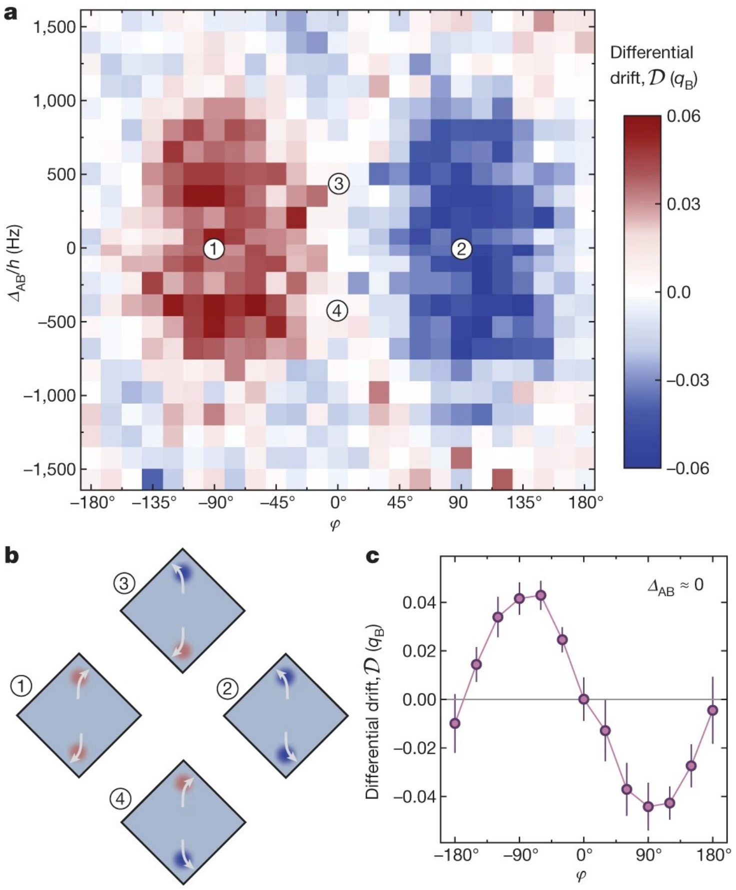

G. Jotzu, et al., Nature **515**, 237 (2014)

Measuring the Chern number

High precision measurement of the Chern number in the Harper-Hofstadter model implemented with laser-assisted tunneling, Aidelsburger et al., Nat. Phys. **11**, 162 (2015)

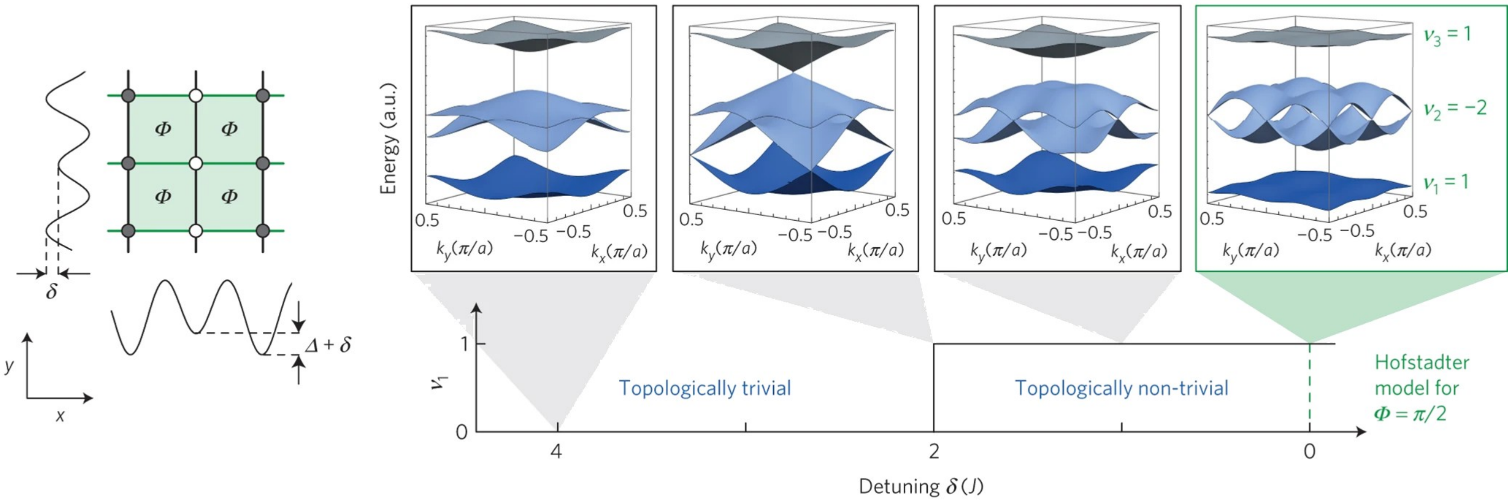

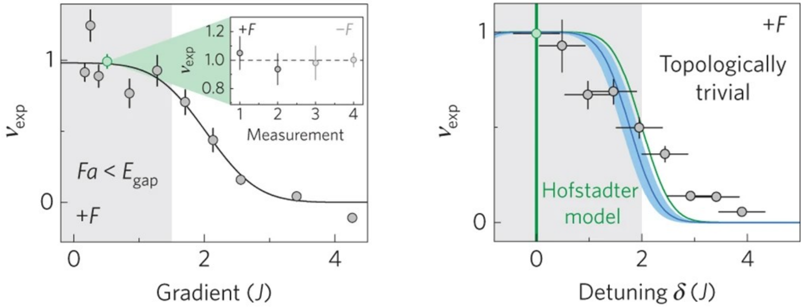

Measured Chern number

$\nu_{exp} = 0.99(5)$

Visualization of skipping orbits with synthetic dimensions

The hard wall boundary conditions along the synthetic dimension enable the observation of skipping orbits

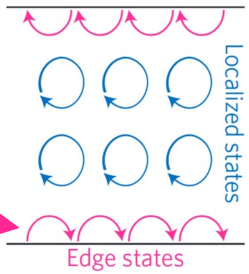

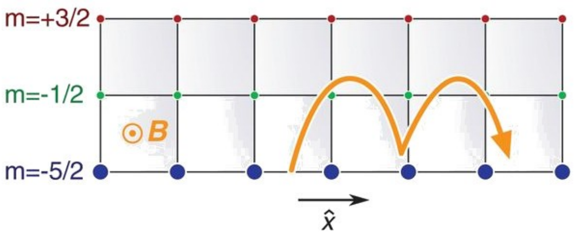

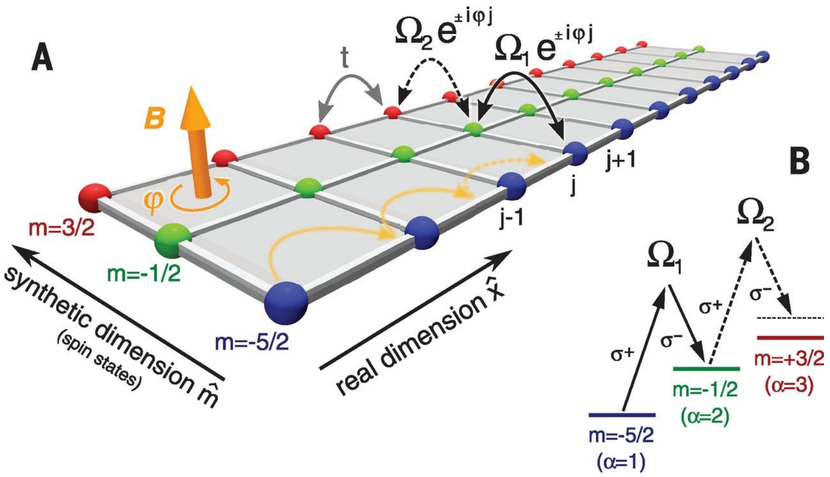

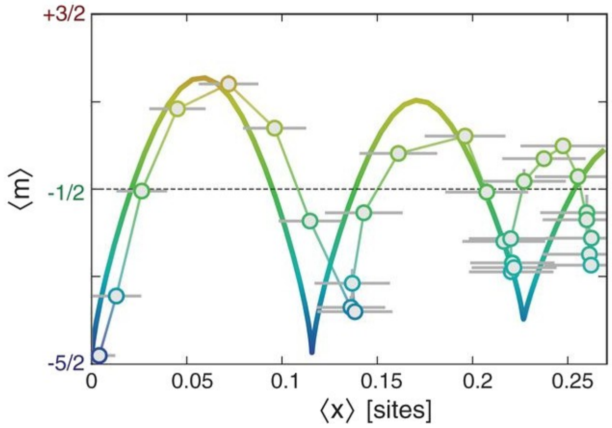

From Mancini et al., Science **349**, 1510 (2015)

See also Stuhl et al., Science **349**, 1514 (2015)

5) Towards the fractional quantum Hall effect with ultracold gases

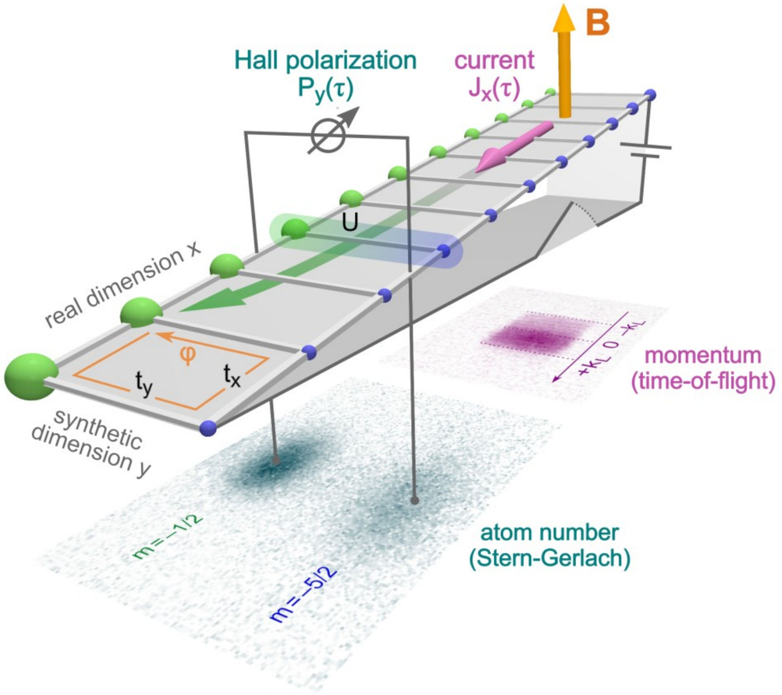

Chern insulators: integer vs. fractional

Chern insulator: quantization of Hall conductance without Landau levels (uniform magnetic field), lattice analogue of quantum Hall effect (e.g. Haldane model)

Integer Chern insulator:

- Fully filled isolated band with nonzero Chern number (done with UG)

Fractional Chern insulator (FCI):

- Nontrivial band topology (as for integer Chern insulator)
- Bandwith much smaller than interaction scale (flat band limit)
- Band geometry: uniform Berry curvature and quantum metric

Long-standing interest to realize the FQHE and FCIs with ultracold gases

Conditions for realizing a fractional Chern insulator

In Landau levels the Berry curvature and the quantum metric are uniform, moreover the trace and determinant conditions are satisfied

Quantum Geometry tensor is positive semidefinite (nonnegative eigenvalues) $\longrightarrow$ $$\frac{1}{2}\mathrm{Tr}[g(\mathbf{k})] \geq \sqrt{\det g(\mathbf{k})} \geq |\Omega(\mathbf{k})|$$

Trace and determinant conditions: inequalities are equalities

FCI are favoured if

- The band is **flat**
- The band is **topologically nontrivial** (nonzero *C*)
- **Uniform Berry curvature** and **quantum metric** (similar to Landau levels)
- Trace and determinant conditions are satisfied (similar to lowest Landau level)

Laughlin wave functions for bosons and fermions

Laughlin wave functions

$$\Psi_m(\{z_i\}) \propto e^{-\frac{1}{4}\sum_j |z_j|^2} \prod_{i<j}^{N} (z_i - z_j)^m$$

m = 2, symmetric w.f., bosons at filling ν = 1/2

m = 3, antisymetric w.f. fermions at filling ν = 1/3

Lattice analogues of Laughlin w.f. for bosons and fermions are found in many lattices (e.g. Haldane and Harper-Hofstadter models) Z. Liu and E. Bergholtz, arXiv:2208.08449

Also lattice analogues of more exotic states (Moore-Read “Pfaffian” state)

Laughlin wave functions in (flattened) Haldane model

T. S. Jackson, M. Gunnar and R. Rahul, Nat. Comm. **6**, 8629 (2015)

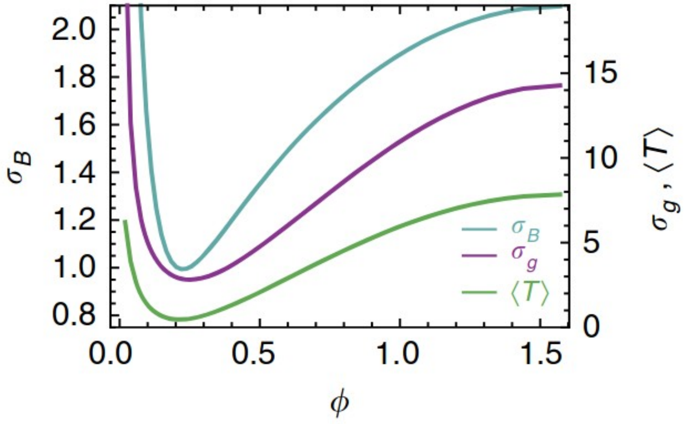

σ_B root mean square of Berry curvature over B.Z.

σ_g root mean square of quantum metric over B.Z.

$\langle T \rangle$ B.Z. average of $T(\mathbf{k}) = \frac{1}{2}\,\mathrm{Tr}\, g(\mathbf{k}) - |\Omega(\mathbf{k})|$

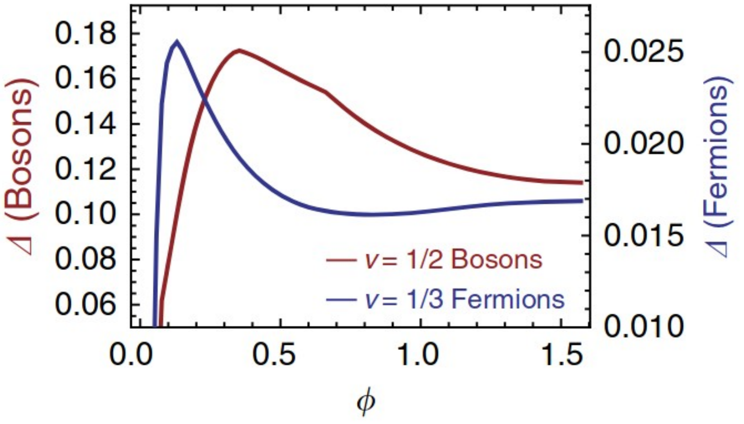

Δ many-body gap for lattice analogue of Laughlin wave functions

The way ahead

- FCI states can be stabilized in a number of lattice models for both bosons and fermions Z. Liu and E. Bergholtz, arXiv:2208.08449

- Advantages of ultracold gases: high tunability of lattice structure and interactions → interesting FCI states (nonabelian), Hamiltonian is known precisely, control and detection at single-atom level with quantum microscopes

- Detection using center of mass drift [J. Motruk and I. Na, Phys. Rev. Lett. **125**, 236401 (2020); C. Repellin et al., Phys. Rev. A **102**, 063316 (2020)]

- Key challenge: realize complex hoppings with minimal heating

- Novel proposal for experiments: dipolar atoms [N. Y. Yao et al., Phys. Rev. Lett. **109**, 266804, (2012)], optical flux lattices [N. R. Cooper, Phys. Rev. Lett. **106**, 175301, (2011)]

- Experiments exploring the interplay of artificial gauge fields in ultracold gases and interactions are under way

Interacting Harper-Hofstadter model in the two-body limit I

Two-leg ladder with nonzero magnetic flux realized with laser-assisted tunneling
Tai et al., Nature **546**, 519 (2017)

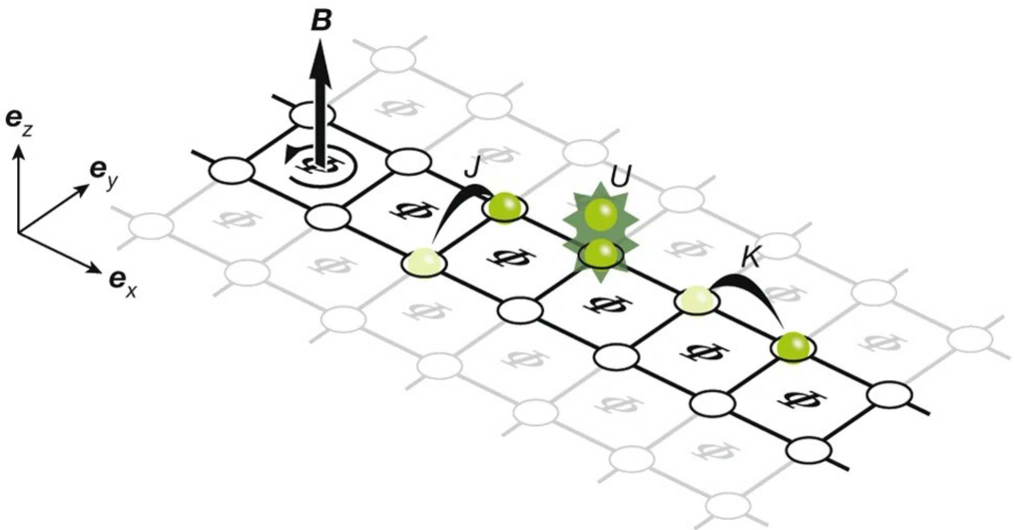

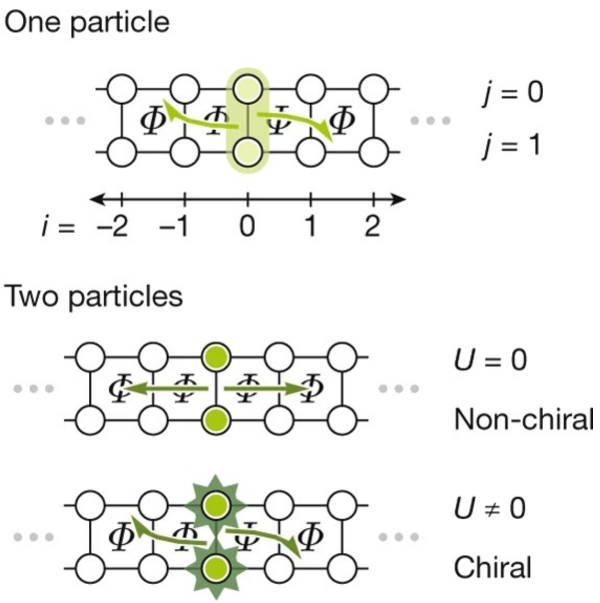

Demonstrated the combined effect of interactions and synthetic gauge fields, and single-atom site-resolved detection and manipulation

Interacting Harper-Hofstadter model in the two-body limit II

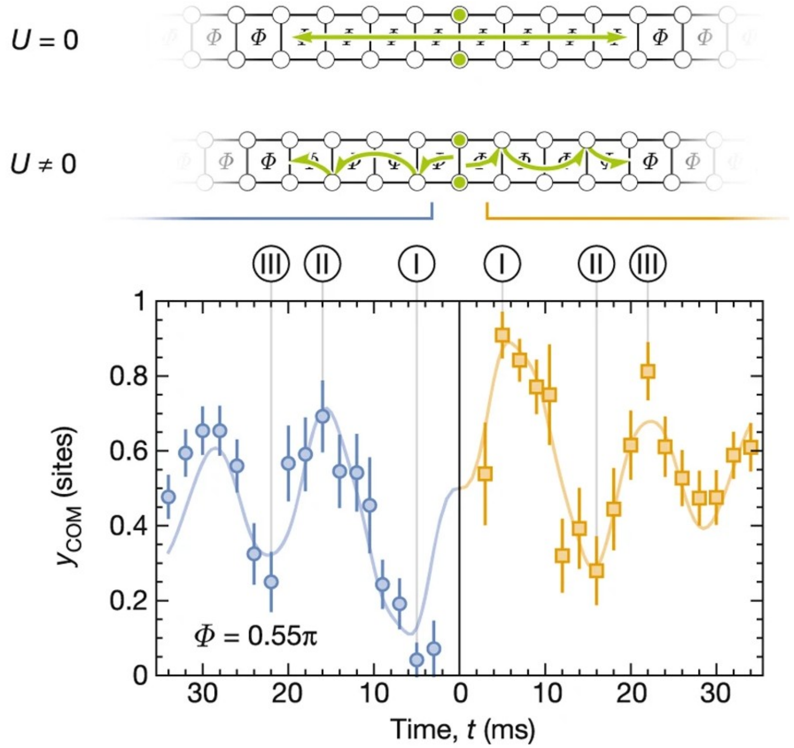

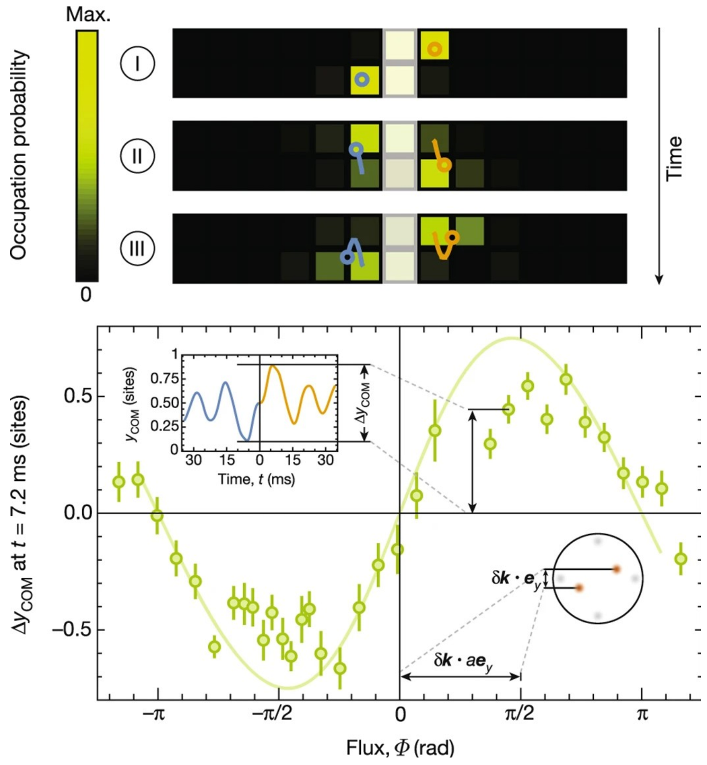

Tai et al., Nature **546**, 519 (2017)

Universal Hall response in a synthetic ladder

Hall imbalance Δ_H
analogous to the Hall coefficient

$$\Delta_{\mathrm{H}} = \left| \frac{P_y}{J_x} \right|$$

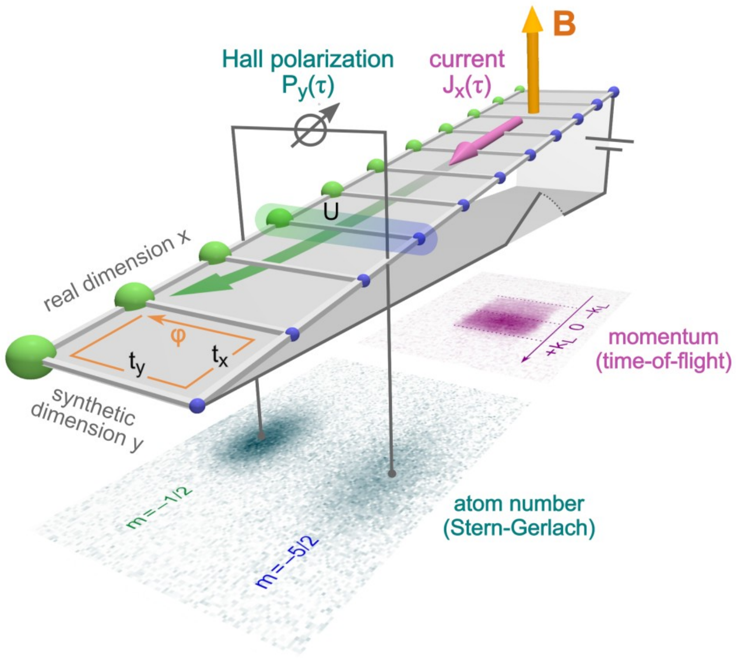

T.-W. Zhou et al., arXiv:2205.13567

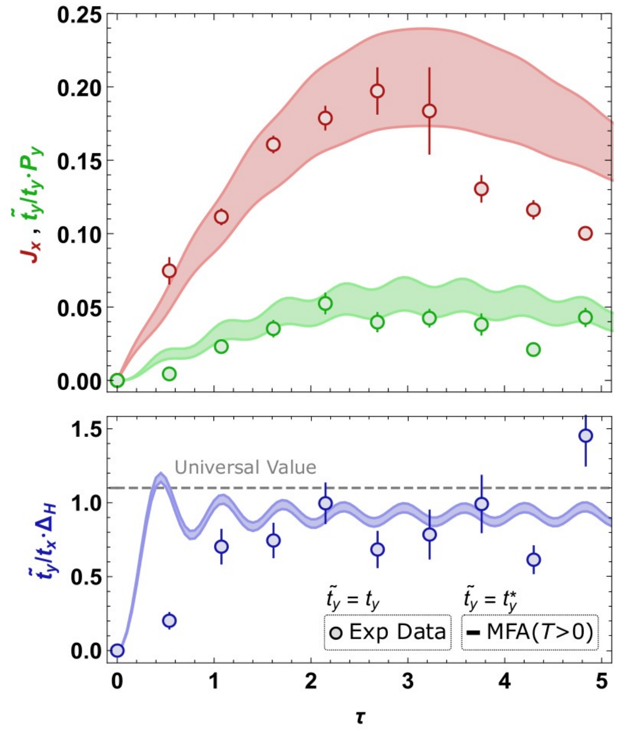

The Hall imbalance acquires a universal value in the presence of interactions S. Greschner et al., Phys. Rev. Lett. **122**, 083402 (2019)

Dressed atomic states and artificial gauge fields

Hamiltonian of an atom (two-internal states) in an optical field

$$\hat{H} = \frac{\hat{\mathbf{p}}^2}{2m} + V\hat{M}(\mathbf{r})$$

$$\hat{M}(\mathbf{r}) = \begin{pmatrix} M_z(\mathbf{r}) & M_x(\mathbf{r}) - iM_y(\mathbf{r}) \\ M_x(\mathbf{r}) + iM_y(\mathbf{r}) & -M_z(\mathbf{r}) \end{pmatrix}$$

For large *V* the atom follows adiabatically the dressed state with lowest energy

$$\hat{M}(\mathbf{r})\,|\Phi(\mathbf{r})\rangle = -\varepsilon_M(\mathbf{r})\,|\Phi(\mathbf{r})\rangle$$

Effective Hamiltonian in the adiabatic approximation

$$\hat{H}_{\text{eff}} = \frac{(\hat{\mathbf{p}} - q\mathbf{A}_{\text{eff}}(\mathbf{r}))^2}{2m} + V_{\text{eff}}(\mathbf{r})$$

$$q\mathbf{A}_{\text{eff}}(\mathbf{r}) = i\hbar\,\langle\Phi(\mathbf{r})|\boldsymbol{\nabla}\Phi(\mathbf{r})\rangle$$

$$n_\phi(\mathbf{r}) = \frac{qB_{\text{eff}}(\mathbf{r})}{h} = \frac{q}{h}\boldsymbol{\nabla}\times\mathbf{A}_{\text{eff}}(\mathbf{r})$$

Local flux number density

For smooth vector potential average flux density is small

$$\bar{n}_\phi \sim \frac{1}{L\lambda}$$

L typical system size
λ laser wavelength

Theoretical proposal: optical flux lattices

Synthetic magnetic fields have been realized with dressed states
Y.-J. Lin et al., Nature **462**, 628 (2009)

To reach the regime of high flux density one has to allow for singularities in the vector potential (similar to Dirac strings for magnetic monopoles) N. R. Cooper, PRL **106**, 175301 (2011)

Chern number = number of flux quanta per unit cell

Large average flux density $\bar{n}_\phi = \frac{C}{\lambda^2}$

Local Bloch vector

$$\mathbf{n}(\mathbf{r}) = \langle \Phi(\mathbf{r}) | \boldsymbol{\sigma} | \Phi(\mathbf{r}) \rangle$$

$$n_\phi(\mathbf{r}) = -\frac{1}{8\pi} \epsilon^{ijk} \epsilon^{\mu\nu} n_i(\mathbf{r}) \partial_\mu n_j(\mathbf{r}) \partial_\nu n_k(\mathbf{r})$$

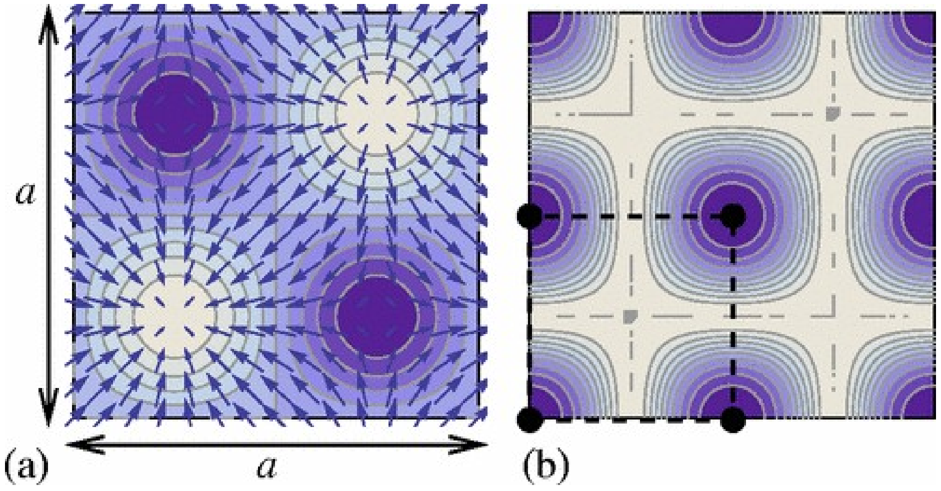

Bloch vector

Flux density

Thanks for your attention!

References

- N. Goldman, J. C. Budich, and P. Zoller, *Topological quantum matter with ultracold gases in optical lattices*, Nature Physics **12**, 639 (2016).

- P. Hauke and I. Carusotto, *Quantum Hall and Synthetic Magnetic-Field Effects in Ultra-Cold Atomic Systems,* arXiv:2206.07727 (Invited Contribution to Encyclopedia of Condensed Matter Physics, 2nd edition)

- N. Goldman, G. Juzeliunas, P. Öhberg, and I. B. Spielman, *Light-induced gauge fields for ultracold atoms*, Reports on Progress in Physics **77**(12), 126401 (2014)

- N. R. Cooper, J. Dalibard and I. B. Spielman, *Topological bands for ultracold atoms*, Reviews of Modern Physics **91**, 015005 (2019)

- André Eckardt, *Colloquium: Atomic quantum gases in periodically driven optical lattices*, Review of Modern Physics **89**, 011004 (2017)

- N. R. Cooper, *Rapidly rotating atomic gases*, Advances in Physics **57**, 539 (2008)

- S. A. Parameswaran, R. Roy and S. L. Sondhi, *Fractional quantum Hall physics in topological flat bands*, C. R. Physique **14**, 816 (2013).

References (continued)

- E. J. Bergholtz and Z. Liu, *Topological flat band models and fractional Chern insulators*, Int. J. Mod. Phys. B **27**, 1330017 (2013)
- Z. Liua and E. J. Bergholtz, *Recent Developments in Fractional Chern Insulators*, arXiv:2208.08449